Journal of Peptide Science
J. Peptide Sci. **9**: 212–220 (2003)
Published online in Wiley InterScience (www.interscience.wiley.com). DOI: 10.1002/psc.447

JOURNAL OF PEPTIDE SCIENCE

Effects of Detergents on the Secondary Structures of Prion Protein Peptides as Studied by CD Spectroscopy

YOSHIHIRO KURODA,* YOSHITAKA MAEDA, SHINICHI SAWA, KIYOHIRO SHIBATA, KAZUHIDE MIYAMOTO and TERUMICHI NAKAGAWA

Graduate School of Pharmaceutical Sciences, Kyoto University, Kyoto, 606-8501, Japan

Received 3 September 2002
Accepted 10 October 2002

Abstract: Pathogenic prion proteins (PrP^{Sc}) are thought to be produced by α-helical to β-sheet conformational changes in the normal cellular prion proteins (PrP^{C}) located solely in the caveolar compartments. In order to inquire into the possible conformational changes due to the influences of hydrophobic environments within caveolae, the secondary structures of prion protein peptides were studied in various kinds of detergents by CD spectra. The peptides studied were PrP(129–154) and PrP(192–213); the former is supposed to assume β-sheets and the latter α-helices, in PrP^{Sc}. The secondary structure analyses for the CD spectra revealed that in buffer solutions, both PrP(129–154) and PrP(192–213) mainly adopted random-coils (~60%), followed by β-sheets (30%–40%). PrP(129–154) showed no changes in the secondary structures even in various kinds of detergents such as octyl-β-D-glucopyranoside (OG), octy-β-D-maltopyranoside (OM), sodium dodecyl sulfate (SDS), Zwittergent 3–14 (ZW) and dodecylphosphocholine (DPC). In contrast, PrP(192–213) changed its secondary structure depending on the concentration of the detergents. SDS, ZW, OG and OM increased the α-helical content, and decreased the β-sheet and random-coil contents. DPC also increased the α-helical content, but to a lesser extent than did SDS, ZW, OG or OM. These results indicate that PrP(129–154) has a propensity to adopt predominantly β-sheets. On the other hand, PrP(192–213) has a rather fickle propensity and varies its secondary structure depending on the environmental conditions. It is considered that the hydrophobic environments provided by these detergents may mimic those provided by gangliosides in caveolae, the head groups of which consist of oligosaccharide chains containing sialic acids. It is concluded that PrP^{C} could be converted into a nascent PrP^{Sc} having a transient PrP^{Sc} like structure under the hydrophobic environments produced by gangliosides.

Keywords: α-helix; β-sheet; octylglucopyranoside; octylmaltopyranoside; sodium dodecyl sulfate (SDS); dodecylphosphocholine (DPC); Zwittergent 3–14 (ZW); prion protein

INTRODUCTION

Creutzfeldt–Jakob disease, kuru, Gerstmann–Sträussler–Scheinker (GSS) disease and fatal familial insomnia in human beings, as well as scrapie and bovine spongiform encephalopathy in animals, are fatal neurodegenerative diseases that form part of the group of transmissible spongiform encephalopathies, also known as prion diseases [1–3]. Transmissible spongiform encephalopathies feature the accumulation, primarily in the brain, of the glycoprotein PrP^{Sc}, which is a conformationally altered isoform of a normal cellular protein (PrP^{C}) of the host [1–3]. No covalent differences have been found to distinguish the two PrP isoforms [4]. The conversion seems to involve a conformational change in which the α-helical content decreases while the amount of β-sheets increases dramatically [5]. Prion replication seems to be dependent on the interaction between the host PrP^{C} and the

*Correspondence to: Dr Yoshihiro Kuroda, Graduate School of Pharmaceutical Sciences, Kyoto University, Kyoto, 606-8501, Japan; e-mail: yokuroda@pharm.kyoto-u.ac.jp

pathogenic PrP^{Sc}. It is argued that an auxiliary molecule mediates the replication [6]. Kaneko *et al.* have shown the binding sites of the auxiliary molecule, named 'protein X' [7]; the sites locate at the *C*-terminal half side of PrP^{C} [8] (Figure 1A). It is noticed that the formation of PrP^{Sc} is primarily due to conformational changes from α-helices to β-sheets of PrP^{C}. In the β-sheets, the side-chains of the constituent amino acids align in the same directions. Thus in aqueous solutions, hydrophobic surfaces are expected to assist in creating a seed of β-sheet structure for PrP^{C} or to facilitate the formation of PrP^{Sc} by interacting with the hydrophobic amino acids of PrP^{C} or PrP^{Sc}. Saccharide chains are one of the candidates that offer such hydrophobic surfaces [9].

PrP^{C} is GPI(glycosylphosphatidylinositol)-anchored at its S231 (Syrian hamster, Figure 1A) [10] in caveolar compartments [11]. The pathogenic PrP^{Sc} is considered to be produced solely in the caveolae [12–14]. The caveolae are endocytic compartments in endothelial cells, in which a molecule is moved across the cell by transcytosis [11]. The caveolae are full of sphingomyelin, cholesterol and sphingoglycolipids known as gangliosides. The PrP has two Asn-linked saccharide chains at N181 and N197 (Syrian

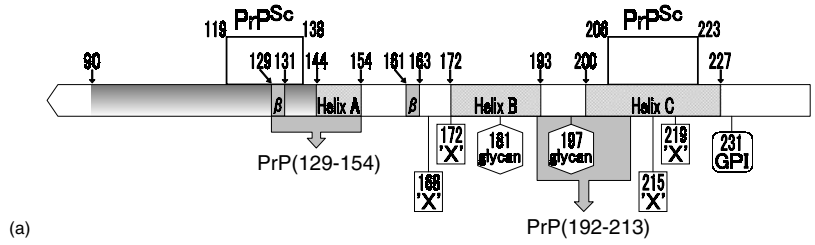

PrP(129-154)
Ac M L G S A M S R P M M H F G N D W E D R Y Y R E N M NH_2

PrP(192-213)
(b) Ac T T K G E N F T E T D I K I M E R V V E Q M NH_2

Figure 1 (A) Schematic representation of the Syrian hamster prion protein sequence. The locations of three α-helices (helix A, helix B and helix C), two β-sheets (β), two glycosylation sites (glycan), 'protein X' binding sites ('X'), the site of GPI-anchor (GPI) and putative PrP^{Sc} binding sites (PrP^{Sc}) are indicated. (B) The amino acid sequences of PrP(129–154) and PrP(192–213); their *N*-termini were acetylated (Ac–) and their *C*-termini were amidated (–NH_2).

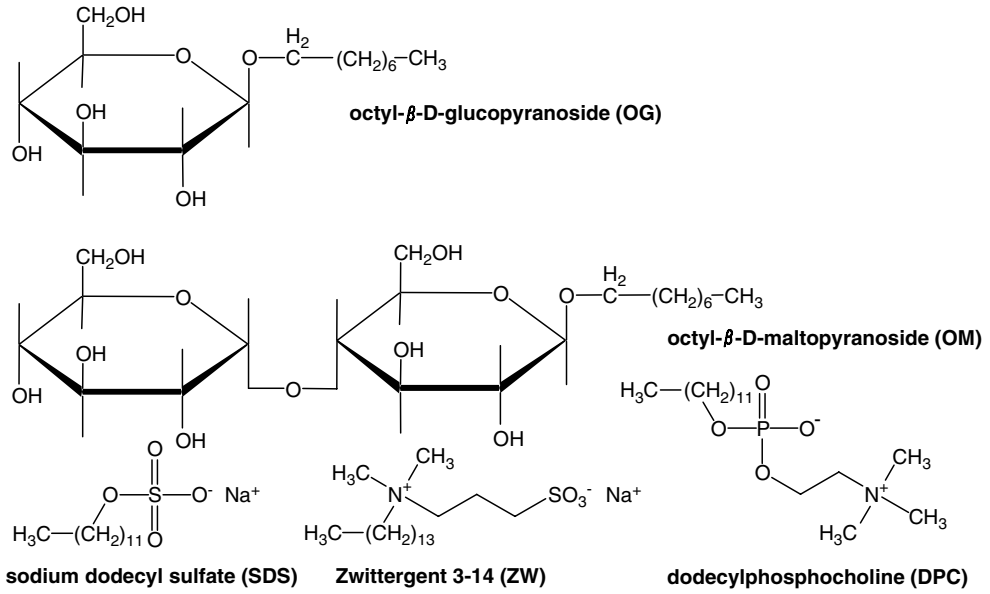

Figure 2 The structure of octyl-β-D-glucopyranoside (OG), octy-β-D-maltopyranoside (OM), sodium dodecyl sulfate (SDS), Zwittergent 3–14 (ZW) and dodecylphosphocholine (DPC).

hamster, Figure 1A) [15, 16]. Accordingly, PrP^{C}s in caveolae are surrounded by complex hydrophobic surfaces provided by hydrocarbon chains, cholesterol and saccharide chains. These hydrophobic environments could work as an, as yet, unidentified 'protein X' [17].

In order to inquire into a possible transformation from PrP^{C} to a pathogenic PrP^{Sc} by interactions with the hydrophobic surfaces in caveolae, the secondary structures of prion protein peptides were studied in various kinds of detergents by CD spectroscopy (Figure 2). The amino acid sequence of the Syrian hamster prion protein was followed [18], because its normal cellular form of the structure is well determined by NMR spectroscopy [19]. The peptides studied were taken from the major structural parts of PrP^{C}, i.e. PrP(129–154) and PrP(192–213) (Figure 1B). The former includes a β-sheet and an α-helical region in PrP^{C} [19]. Both are speculated to be converted to β-sheets in PrP^{Sc} [20, 21]. The latter includes an α-helical region in PrP^{C} and locates near the 'protein X' binding sites (Figure 1A). The secondary structure of this α-helical part is speculated to be retained as it is, even when PrP^{C} is converted to PrP^{Sc} [20, 21].

MATERIALS AND METHODS

Materials

Octyl-β-D-glucopyranoside (OG) and octy-β-D-maltopyranoside (OM) were obtained from Tokyo Kasei (Tokyo, Japan) and Sigma (St Louis, MO), respectively. Sodium dodecyl sulfate (SDS) was obtained from Nacalai Tesque (Kyoto, Japan) and dodecylphosphocholine (DPC) was obtained from Avanti Polar-Lipids (Alabaster, Alabama). Zwittergent 3–14 (n-tetradecyl-N,N-dimethyl-3-ammonio-1-propanesulfonate; ZW) was obtained from Calbiochem (San Diego, CA). Peptides, PrP(129–154) and PrP(192–213), were synthesized automatically by solid-phase methods, using 9-fluorenylmethoxycarbonyl (Fmoc) chemistry on an Applied Biosystems 433A peptide synthesizer; their *N*-termini were acetylated, and their *C*-termini were amidated. After cleavage with trifluoroacetic acid (TFA), the peptides were purified on a reverse-phase C_{18} HPLC column using a gradient of 70% A: 30% B to 50% A: 50% B, where A is 0.1% TFA in water and B is 0.1% TFA in acetonitrile; the rate of decrease in A was 20%/40 min. The peptides were characterized by ion-spray mass spectrometry on a Perkin-Elmer SCIEX API III mass spectrometer: PrP(129–154), m/z calcd 3264.3820 (monoisotope), 3266.7368 (average), found 1634.5 ($[M + 2H]^{2+}$), 1090.0 ($[M + 3H]^{3+}$); PrP(192–213), m/z calcd 2639.2935 (monoisotope), 2641.0230 (average), found 1321.0 ($[M + 2H]^{2+}$), 881.5 ($[M + 3H]^{3+}$).

CD Spectra

A weighed amount of the peptide (50 μM) dissolved in an isotonic (310 mOsm, 120 mM) phosphate buffer without or with 0.5% ~3.0% OG, 0.5% ~6.0% OM, 0.03% ~1.0% SDS, 0.003% ~0.1% ZW or 0.03% ~0.50% DPC was subjected to measurement of CD spectra. The detergent solutions were prepared by using the isotonic phosphate buffer. The range of the concentrations studied was determined by taking into account the following critical micelle concentration (cmc) of each detergent. The cmc values reported are: OG, 19–25 mM (0.55%–0.73%) [22]; OM, 23.4 mM (1.06%) [23]; SDS, 1.2–7.1 mM (0.035%–0.20%) [22]; ZW, 0.1–0.4 mM (0.0036%–0.015%) [24]; and DPC, 1.1–1.5 mM (0.039%–0.053%) [22]. The cmc values in the present sample solutions, however, would be lower than these values because of the use of isotonic phosphate buffer with a high salt concentration [25]. The CD spectra (190–250 nm) were measured on a Jasco J-720 spectrometer interfaced to an NEC PC-9801 microcomputer or on a Jasco J-820 spectrometer interfaced to a microcomputer with Microsoft Windows 95 operating systems. A 0.5 mm pathlength quartz cell was used for a 50 μM sample solution. Eight scans were averaged for each sample; the averaged blank spectra of detergents dissolved into the same buffer solutions were subtracted. The vertical scale of the CD spectra was expressed as a mean residue ellipticity in units of deg·cm^2/dmol. The percentages of each secondary structure were analysed by using CONTIN/LL within the CDPro software package [26, 27]; the fraction of turns was included in the percentage of random-coils for convenience.

RESULTS

Effects of OG and OM on the Secondary Structures of PrP(129–154) and PrP(192–213)

Both OG and OM are non-ionic detergents (Figure 2); their cmc values are 0.55%–0.73% [22]

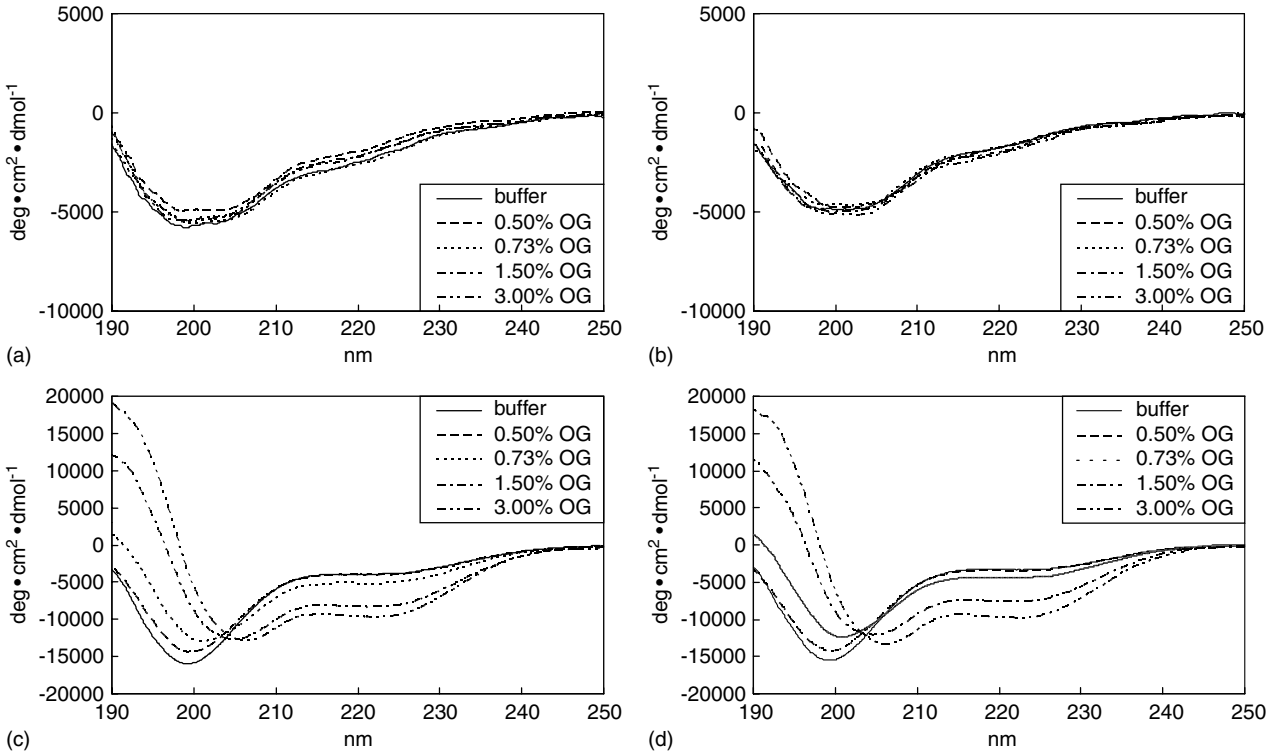

Figure 3 CD spectra of PrP(129–154) (A, B) and PrP(192–213) (C, D) without and with 0.50%, 0.73%, 1.50% and 3.00% OG. (A) and (C) were observed immediately after preparing sample solutions, whereas (B) and (D) were observed 1 week later.

and 1.06% [23], respectively. Figure 3 shows the CD spectra of PrP(129–154) (A and B) and PrP(192–213) (C and D) in isotonic phosphate buffer and in 0.5%, 0.73%, 1.5% and 3.0% OG solutions. The spectra shown in (A) and (C) were observed immediately after preparing the sample solutions, whereas those shown in (B) and (D) were observed 1 week later. Typical secondary structures (α-helices, β-sheets and random-coils) of a protein or a peptide are known to be well-characterized according to the following CD spectral patterns [28]. α-Helices show double-negative maxima at 208–210 (π-π^* transitions) and 222 nm (n-π^* transitions) and a strong positive maximum at 191–193 nm (π-π^* transitions). β-Sheets show a negative band near 216–218 nm and a positive one near 195–200 nm. Random-coils generally show a strong negative band near 200 nm and a very weak band around 220 nm, which can be either a positive band or a negative shoulder. Inspection of Figure 3A tells us that PrP(129–154) in buffer essentially assumes random-coils. No appreciable spectral changes were noted with increasing concentrations of OG or on standing the solutions for 1 week (Figure 3B). In contrast, although PrP(192–213) in buffer also assumed random-coils, the spectral pattern drastically changed with increasing concentrations of OG (Figure 3C). The negative band near 205–225 nm was clearly increased, while the maximum at 190 nm was greatly increased toward a positive value. These spectral changes almost converged at 1.5%–3.0% OG and resulted in a typical α-helical spectral pattern. Again, no spectral changes could be seen in each spectrum on standing the solutions for 1 week (Figure 3D). These observations indicate that the interaction between PrP(192–213) and OG rapidly stabilized the structure of PrP(192–213) to adopt α-helices. In order to analyse secondary structure fractions due to α-helices, β-sheets and random-coils, the secondary structures were analysed using CONTIN/LL in the CDPro software package [26, 27]. Calculations were made for the CD spectra shown in Figure 3A and C, because essentially no spectral changes were seen even on standing the solutions for 1 week. The results are summarized in Table 1. Notably, the CONTIN/LL revealed that PrP(129–154) involves 37%–39% β-sheets, regardless of the concentration of OG. In

Table 1 Secondary Structure Analysis for the CD spectra of PrP(129–154) and PrP(192–213) in OG, OM, SDS, ZW and DPC Solutions

Concentration (%)		PrP(129–154)			PrP(192–213)		
		α-Helix (%)	β-Sheet (%)	Random coil (%)	α-Helix (%)	β-Sheet (%)	Random coil (%)
OG	0.00	5.8	37.1	57.0	10.2	27.9	61.9
	0.50	5.3	39.0	55.7	11.0	27.4	61.6
	0.73	6.0	37.0	57.0	17.7	25.3	57.1
	1.50	5.7	38.9	55.5	29.9	16.1	53.9
	3.00	5.7	38.6	55.7	36.8	12.8	50.4
OM	0.00	5.8	37.1	57.0	10.2	27.9	61.9
	0.50	5.8	37.4	56.9	7.3	31.3	61.4
	1.06	5.7	38.1	56.1	14.6	28.9	56.5
	1.50	5.6	37.9	56.5	18.0	27.8	54.2
	6.00	5.8	38.9	55.5	45.6	8.8	45.7
SDS	0.00	5.8	37.1	57.0	10.2	27.9	61.9
	0.03	5.1	42.1	52.8	19.8	23.2	56.9
	0.20	5.0	43.6	51.5	37.2	14.4	48.2
	1.00	5.3	39.9	54.9	41.3	12.8	45.8
ZW	0.000	5.8	37.1	57.0	10.2	27.9	61.9
	0.003	4.1	40.9	54.9	11.3	27.6	61.0
	0.015	4.4	40.5	55.1	7.5	27.4	65.2
	0.100	6.8	40.3	53.0	42.5	8.9	48.6
DPC	0.00	5.8	37.1	57.0	10.2	27.9	61.9
	0.03	4.1	41.5	54.4	8.1	27.8	64.2
	0.06	5.2	41.4	53.5	11.1	27.1	61.9
	0.10	5.1	40.1	54.9	17.7	23.0	59.4
	0.50	6.4	40.1	53.5	34.2	14.4	51.5

contrast, the α-helical content of PrP(192–213) increased with increasing concentrations of OG as implied from changes in the shape of the CD spectra. The CONTIN/LL showed that the increase in the α-helical content was compensated for by the decrease in both the β-sheet and the random-coil contents.

Figure 4 shows the CD spectra of PrP(129–154) (A and B) and PrP(192–213) (C and D) in isotonic phosphate buffer and in 0.5%, 1.06%, 1.50% and 6.00% OM solutions. The spectra shown in (A) and (C) were observed immediately after preparing the sample solutions, while those shown in (B) and (D) were observed 1 week later. As shown in Figure 4A, no differences in the CD spectra could be seen between PrP(129–154) in OG and that in OM. Also, no time-dependent alterations in the spectra were noted between Figures 4A and B. PrP(192–213) showed similar behaviour to that seen in OG with increasing concentrations of OM (Figure 4C). The CD spectrum converged to that due to the α-helices at 6.00% OM. Again, no time-dependent alterations in the spectra were noted between Figures 4C and D. The CONTIN/LL calculations for the spectrum shown in Figure 4A gave similar values to those calculated in OG solutions, as expected, whereas for the spectrum shown in Figure 4C, they gave a little larger α-helical content than for the corresponding spectrum in OG. The increase in the α-helical content was compensated for by the decrease in the random-coil value (Table 1).

Effects of SDS on the Secondary Structures of PrP(129–154) and PrP(192–213)

In order to investigate the effects of a charge at the hydrophilic head of detergents, the CD spectra of the peptides in SDS solutions were observed. In the following, all the CD spectra were recorded immediately after preparing the sample solutions, since no time-dependent changes in the secondary structure were noted in OG and OM. The SDS is an ionic detergent having a negative charge at

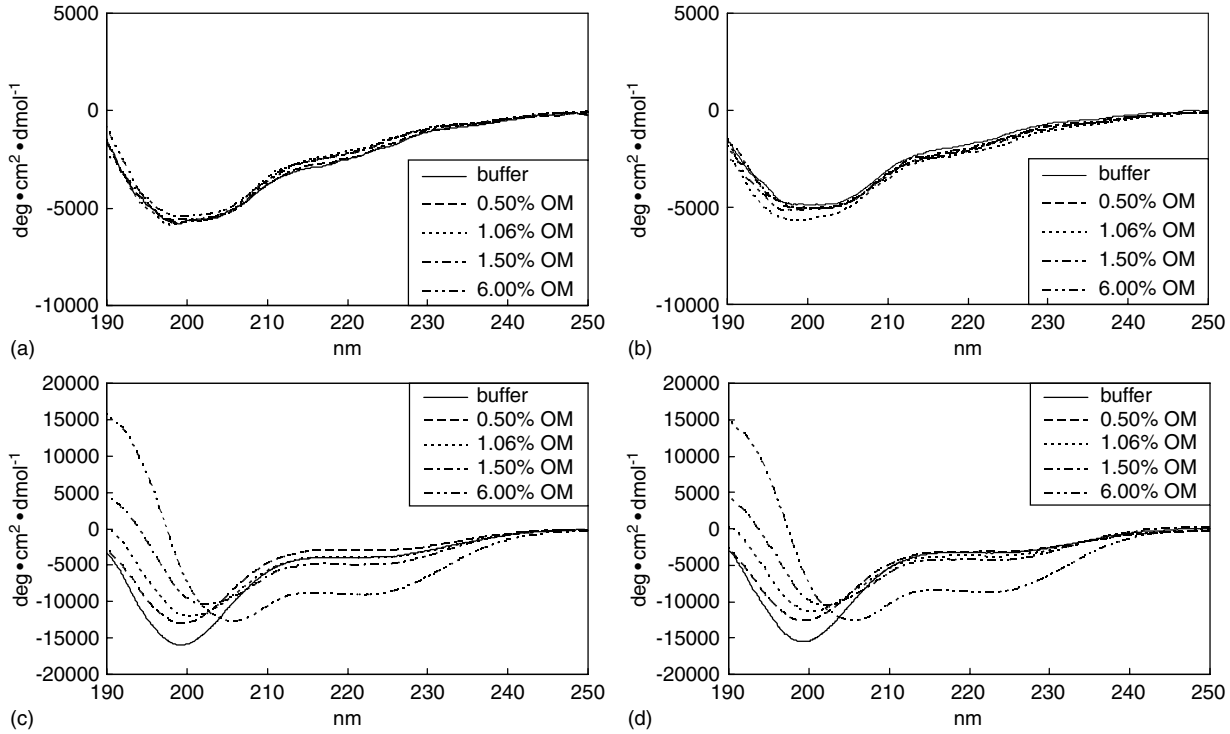

Figure 4 CD spectra of PrP(129–154) (A, B) and PrP(192–213) (C, D) without and with 0.50%, 1.06%, 1.50% and 6.00% OM. (A) and (C) were observed immediately after preparing sample solutions, whereas (B) and (D) were observed 1 week later.

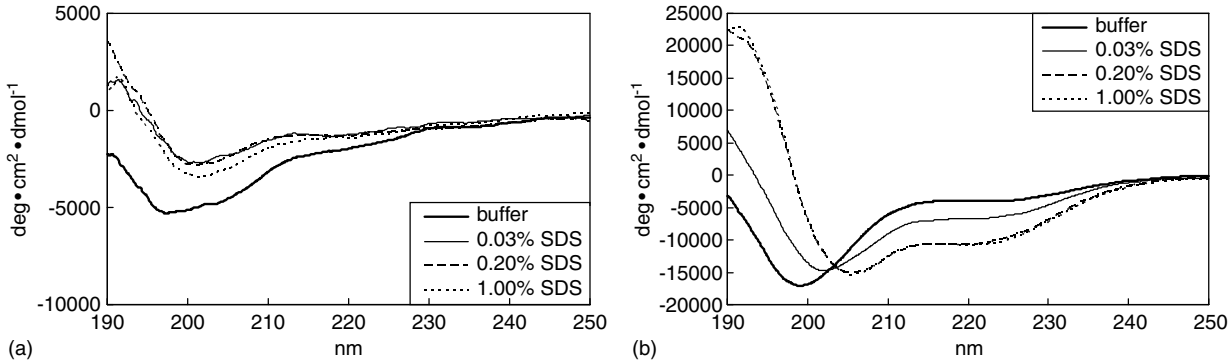

Figure 5 CD spectra of PrP(129–154) (A) and PrP(192–213) (B) without and with 0.03%, 0.20% and 1.00% SDS.

the polar head group (Figure 2); its cmc value is 0.035%–0.20% [22]. Figure 5 shows the CD spectra of PrP(129–154) and PrP(192–213) in isotonic phosphate buffer and in 0.03%, 0.20% and 1.00% SDS solutions. The CD spectra of PrP(129–154) in SDS were rather featureless compared with those in OG or OM. However, the spectral pattern was essentially due to random-coils. The CONTIN/LL gave similar secondary structure fractions for β-sheets and random-coils, respectively, to those for OG or OM (Table 1). However, differences in the CD spectra from those observed in buffer suggest that in contrast to OG or OM, SDS caused some change or other in the secondary structure of PrP(129–154). On the other hand, the CD spectra of PrP(192–213) plainly converged into those due to α-helices. Moreover, the increased ellipticities of the double-negative maxima indicate that the α-helical content was larger than that attained in OG or OM solution. The CONTIN/LL calculations clearly followed these spectral changes: the α-helical content was increased greatly up to ~41%, while fractions due to β-sheets and random-coils were markedly decreased.

Effects of ZW and DPC on the Secondary Structures of PrP(129–154) and PrP(192–213)

The high α-helical content of PrP(192–213) in SDS solutions suggested that the negative charge at the polar head group of SDS played an important role in stabilizing the α-helical structure. In order to see the effects of the negative charge at the head group of detergents, ZW and DPC were investigated further. Both ZW and DPC are ionic detergents having one positive and one negative charge at their head groups, but the total charge of the molecule is neutral (Figure 2). The locations of the positive and the negative charges are different; in ZW, there is a negative charge at the terminal of the head, whereas in DPC, there is a positive charge at the corresponding terminal position. Their cmc values are 0.0036%–0.015% for ZW [24] and 0.039%–0.053% for DPC [22].

Figure 6 shows CD spectra of PrP(129–154) and PrP(192–213) in isotonic phosphate buffer and in 0.003%, 0.015% and 0.1% ZW solutions. The CD spectra of PrP(129–154) at 0.003% and 0.015% ZW were more unstructured than those seen in SDS, but the spectrum at 0.1% ZW explicitly suggested the presence of β-sheets. The changes in the CD spectra of PrP(192–213) were more dramatic at 0.1% ZW than those seen in Figure 6A. Although any indications of the changes in the secondary structure were not recognized by the CD spectra at 0.003% and 0.015% ZW, the spectrum changed abruptly into α-helices at 0.1% ZW. The CONTIN/LL calculations showed a nearly identical α-helical content to that for PrP(192–213) at 1.0% SDS (Table 1).

Figure 7 shows the CD spectra of PrP(129–154) and PrP(192–213) in isotonic phosphate buffer and in 0.03%, 0.06%, 0.10% and 0.50% DPC solutions. The CD spectra of PrP(129–154) in DPC were also unstructured as in the case of SDS or in the case of ZW at 0.003% and 0.015%, but were definitely different from those recorded in buffer. The spectral patterns still suggest that PrP(129–154) predominantly assumed random-coils. The CONTIN/LL calculations gave similar secondary structure fractions to those calculated for the other detergents. Any indications in the changes in the secondary structures were not recognized by the CD spectrum of PrP(192–213) in the concentration range 0.03%–0.06%; however, it was inclined to increase

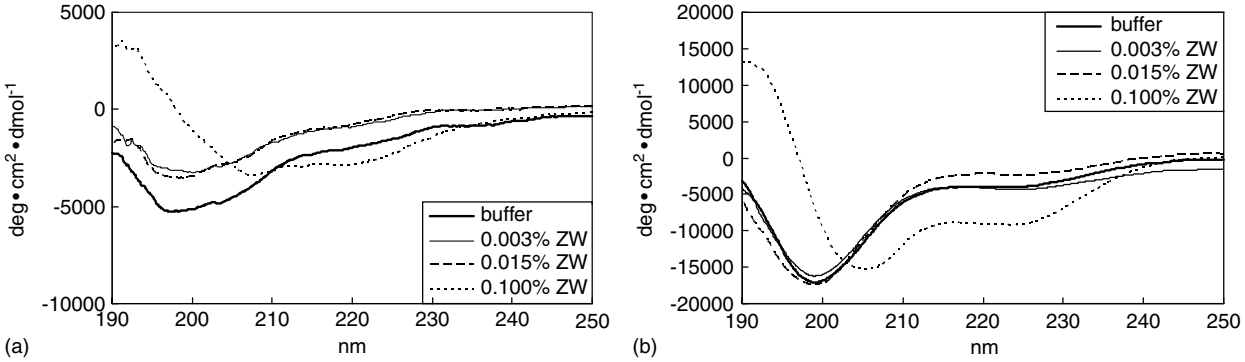

Figure 6 CD spectra of PrP(129–154) (A) and PrP(192–213) (B) without and with 0.003%, 0.015% and 0.100% ZW.

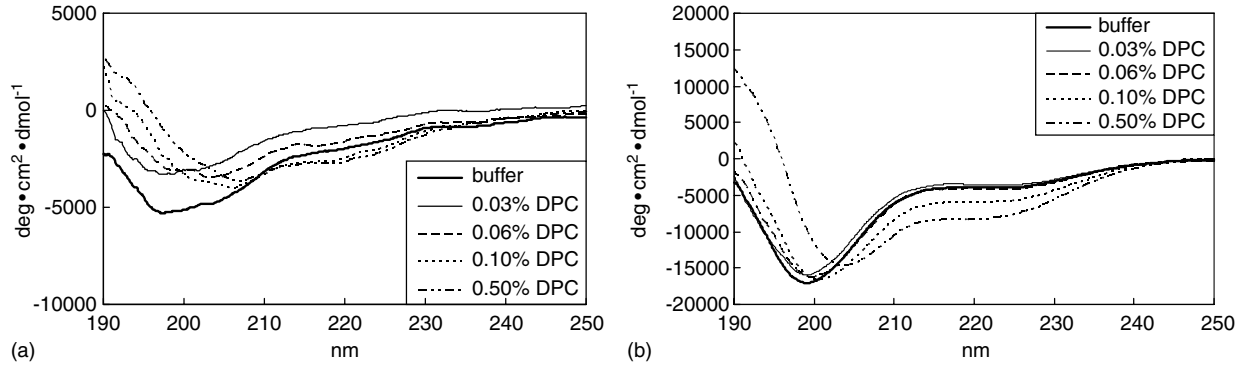

Figure 7 CD spectra of PrP(129–154) (A) and PrP(192–213) (B) without and with 0.03%, 0.06%, 0.10% and 0.50% DPC.

the α-helical structure beyond 0.10% DPC. The CONTIN/LL calculations followed well these trends. These results show that a detergent having a negative charge at its hydrophilic head has a propensity to stabilize α-helices of PrP(192–213).

DISCUSSION

According to Liu *et al.* the recombinant Syrian hamster prion protein contains three α-helices at regions spanning D144–M154 (helix A), Q172–T193 (helix B) and E200–D227 (helix C) and two short anti-parallel β-strands for the residues M129–G131 and V161–Y163 [19] (Figure 1A). An analogous NMR structure has also been reported by Riek *et al.* for the recombinant mouse prion protein MoPrP(121–231) [29]. In contrast, no structure determinations have been made for PrP^{Sc}. Pan *et al.* showed that α-helix and β-sheet contents change from 42% α-helix and 3% β-sheet in PrP^{C} to 30% α-helix and 43% β-sheet in PrP^{Sc} for the materials purified from normal and scrapie-infected Syrian hamster brains [5]. Safar *et al.* also reported the secondary structure of PrP^{Sc} purified from golden Syrian hamsters and then reconstituted into liposomes. The secondary structure contents obtained by CD spectra were 20% α-helix, 34% β-sheet and 46% β-turns and random coil [30]. Thus, a high β-sheet content and a low α-helical content are characteristics of PrP^{Sc}. It has been suggested that at least the region 90–145 is converted to β-sheets in PrP^{Sc}, the *C*-terminal helix B and helix C remaining as α-helices [20, 21]. In fact, the peptide 90–145 aggregates to form rod-shaped polymers and caused GSS disease in transgenic mice [31, 32]. The pathogenic PrP^{Sc} is considered to be produced solely in caveolae [12–14]. The GPI-anchored PrP^{C} that binds to 'protein X' in caveolae, is converted to PrP^{Sc} by also interacting with the seed of PrP^{Sc} [7, 17]. The 'protein X' binding sites locate near or on helix B and helix C [7, 8] (Figure 1A). On the other hand, the seed of the PrP^{Sc} binding site was suggested to be regions 119–138 and 206–223 by Horiuchi and Caughey [33] (Figure 1A).

The present results indicate that the detergents tried did not appreciably alter the secondary structure of PrP(129–154), holding the secondary structure as ~40% β-sheets and ~60% random-coils. These findings mean that PrP(129–154) has an intrinsic conformational preference to adopt β-sheets, irrespective of environmental conditions. The Met129–Trp145 moiety in PrP(129–154) overlaps partly with the PrP^{C}–PrP^{Sc} interaction sites [33] and is involved in the region 90–145. Thus, the propensity of the amino acids in region 129–154 studied, which is inclined to adopt β-sheets, may facilitate the conformational transition for the 90–145 region of PrP^{C} into a PrP^{Sc}-like structure by mimicking the β-sheet structure of a neighbouring PrP^{Sc}.

On the contrary, PrP(192–213) adopted various secondary structures: β-sheets in isotonic phosphate buffer, but α-helices in OG, OM, SDS and ZW or weakly in DPC solutions. These findings mean that PrP(192–213) has a rather fickle propensity to adopt various secondary structures depending on the environmental conditions. Hydrophobic environments, especially involving negative charges, may stabilize helix C (200–227) of PrP^{C} and facilitate the binding of 'protein X' to PrP^{C}, since the 'protein X' binding sites one near the 192–213 region studied, i.e. at Thr215 and Gln219 [7, 8] (Figure 1A). The α-helical conformation of helix C, still retained in the nascent PrP^{Sc}, may also be stabilized and would facilitate development of PrP^{Sc}, since a putative PrP^{Sc} binding site with PrP^{C} span the amino acids in helix C (Figure 1A). Those hydrophobic environments could be fully offered by sphingoglycolipids known as gangliosides in caveolae. In gangliosides, an oligosaccharide chain containing sialic acids is attached to ceramide. Thus, it is concluded that at the membrane surface of caveolae, GPI-anchored PrP^{C} could be altered into a nascent PrP^{Sc} having a transient PrP^{Sc}-like structure under the influences of hydrophobic forces and negative electrostatic potentials produced by the oligosaccharide chains of gangliosides.

REFERENCES

1. Prusiner SB. Prion diseases and the BSE crisis. *Science* 1997; **278**: 245–251.
2. Prusiner SB. Molecular genetics and biophysics of prions. *Virus* 1995; **45**: 5–42.
3. Prusiner SB. Molecular biology of prion diseases. *Science* 1991; **252**: 1515–1522.
4. Stahl N, Baldwin MA, Teplow DB, Hood L, Gibson BW, Burlingame AL, Prusiner SB. Structural studies of the scrapie prion protein using mass spectrometry and amino acid sequencing. *Biochemistry* 1993; **32**: 1991–2002.
5. Pan K-M, Baldwin MA, Nguyen J, Gasset M, Serban A, Groth D, Mehlhorn I, Huang Z, Fletterick RJ, Cohen FE, Prusiner SB. Conversion of α-helices into

β-sheets features in the formation of the scrapie prion proteins. *Proc. Natl Acad. Sci. USA* 1993; **90**: 10 962–10 966.
6. Cohen FE, Pan K-M, Huang Z, Baldwin M, Fletterick RJ, Prusiner SB. Structural clues to prion replication. *Science* 1994; **264**: 530–531.
7. Kaneko K, Zulianello L, Scott M, Cooper CM, Wallace AC, James TL, Cohen FE, Prusiner SB. Evidence for protein X binding to a discontinuous epitope on the cellular prion protein during scrapie propagation. *Proc. Natl Acad. Sci. USA* 1997; **94**: 10 069–10 074.
8. Perrier V, Wallace AC, Kaneko K, Safar J, Prusiner SB, Cohen FE. Mimicking dominant negative inhibition of prion replication through structure-based drug design. *Proc. Natl Acad. Sci. USA* 2000; **97**: 6073–6078.
9. Sundari CS, Balasubramanian D. Hydrophobic surfaces in saccharide chains. *Prog. Biophys. Molec. Biol.* 1997; **67**: 183–216.
10. Stahl N, Borchelt DR, Hsiao K, Prusiner SB. Scrapie prion protein contains a phosphatidylinositol glycolipid. *Cell* 1987; **51**: 229–240.
11. Anderson RGW. Caveolae: where incoming and outgoing messengers meet. *Proc. Natl Acad. Sci. USA* 1993; **90**: 10 909–10 913.
12. Taraboulos A, Raeber AJ, Borchelt DR, Serban D, Prusiner SB. Synthesis and trafficking of prion proteins in cultured cells. *Mol. Biol. Cell* 1992; **3**: 851–863.
13. Vey M, Pilkuhn S, Wille H, Nixon R, DeArmond SJ, Smart EJ, Anderson RGW, Taraboulos A, Prusiner SB. Subcellular colocalization of the cellular and scrapie prion proteins in caveolae-like membranous domains. *Proc. Natl Acad. Sci. USA* 1996; **93**: 14 945–14 949.
14. Naslavsky N, Stein R, Yanai A, Friedlander G, Taraboulos A. Characterization of detergent-insoluble complexes containing the cellular prion protein and its scrapie isoform. *J. Biol. Chem.* 1997; **272**: 6324–6331.
15. Haraguchi T, Fisher S, Olofsson S, Endo T, Groth D, Tarentino A, Borchelt DR, Teplow D, Hood L, Burlingame A, Lycke E, Kobata A, Prusiner SB. Asparagine-linked glycosylation of the scrapie and cellular prion proteins. *Arch. Biochem. Biophys.* 1989; **274**: 1–13.
16. Endo T, Groth D, Prusiner SB, Kobata A. Diversity of oligosaccharide structures linked to asparagines of the scrapie prion protein. *Biochemistry* 1989; **28**: 8380–8388.
17. Kaneko K, Vey M, Scott M, Pilkuhn S, Cohen FE, Prusiner SB. COOH-terminal sequence of the cellular prion protein directs subcellular trafficking and controls conversion into the scrapie isoform. *Proc. Natl Acad. Sci. USA* 1997; **94**: 2333–2338.
18. Sticht H, Bayer P, Willbold D, Dames S, Hilbich C, Beyreuther K, Frank RW, Rösch P. Structure of amyloid A4-(1–40)-peptide of Alzheimer's disease. *Eur. J. Biochem.* 1995; **233**: 293–298.
19. Liu H, Farr-Jones S, Ulyanov NB, Llinas M, Marqusee S, Groth D, Cohen FE, Prusiner SB, James TL. Solution structure of Syrian hamster prion protein rPrP(90–231). *Biochemistry* 1999; **38**: 5362–5377.
20. Huang Z, Prusiner SB, Cohen FE. Scrapie prions: a three-dimensional model of an infectious fragment. *Fold. Des.* 1996; **1**: 13–19.
21. Harrison PM, Bamborough P, Daggett V, Prusiner SB, Cohen FE. The prion folding problem. *Curr. Opin. Struct. Biol.* 1997; **7**: 53–59.
22. le Maire M, Champeil P, Moller JV. Interaction of membrane proteins and lipids with solubilizing detergents. *Biochim. Biophys. Acta* 2000; **1508**: 86–111.
23. Mechref Y, Rassi ZE. Comparison of alkylglycoside surfactants in enantioseparation by capillary electrophoresis. *Electrophoresis* 1997; **18**: 912–918.
24. Calbiochem general catalog. 2002; Cat.No. 693017.
25. Tanford C, Reynolds J. Characterization of membrane proteins in detergent solutions. *Biochim. Biophys. Acta* 1976; **457**: 133–170.
26. Sreerama N, Venyaminov SY, Woody RW. Estimation of protein secondary structure from circular dichroism spectra: inclusion of denatured proteins with native proteins in the analysis. *Anal. Biochem.* 2000; **287**: 243–251.
27. Sreerama N, Woody RW. Estimation of protein secondary structure from circular dichroism spectra: comparison of CONTIN, SELCON, and CDSSTR methods with an expanded reference set. *Anal. Biochem.* 2000; **287**: 252–260.
28. Yang JT, Wu C-SC, Martinez HM. Calculation of protein conformation from circular dichroism. *Methods Enzymol.* 1986; **130**: 208–269.
29. Riek R, Wider G, Billeter M, Hornemann S, Glockshuber R, Wüthrich K. Prion protein NMR structure and familial human spongiform encephalopathies. *Proc. Natl. Acad. Sci. USA* 1998; **95**: 11 667–11 672.
30. Safar J, Roller PP, Gajdusek DC, Gibbs Jr CJ. Conformational transitions, dissociation, and unfolding of scrapie amyloid (prion) protein. *J. Biol. Chem.* 1993; **268**: 20 276–20 284.
31. Zhang H, Kaneko K, Nguyen JT, Livshits TL, Baldwin MA, Cohen FE, James TL, Prusiner SB. Conformational transitions in peptides containing two putative α-helices of the prion protein. *J. Mol. Biol.* 1995; **250**: 514–526.
32. Kaneko K, Ball HL, Wille H, Zhang H, Groth D, Torchia M, Tremblay P, Safar J, Prusiner SB, DeArmond SJ, Baldwin MA, Cohen FE. A synthetic peptide initiates Gerstmann-Straussler-Scheinker (GSS) disease in transgenic mice. *J. Mol. Biol.* 2000; **295**: 997–1007.
33. Horiuchi M, Caughey B. Specific binding of normal prion protein to the scrapie form via a localized domain initiates its conversion to the protease-resistant state. *EMBO J.* 1999; **18**: 3193–3203.

